Atmospheric CH4 Dynamics of South-West Bangladesh: A Google Earth Engine-Based Remote Sensing Approach

Tahmid Anam Chowdhury[1,2 *] (tahmidanam@gmail.com),

Nusrat Jahan Ety[3] (nusratjahan.ety40@gmail.com),

Warefta E Murshed[4] (wareftaemurshed@ginearth.org),

Abed Chaudhury[2,5] (kanihati@gmail.com)

[1]Geography and Environment, Shahjalal University of Science and Technology, Sylhet-3114, Bangladesh

[2]Krishan Foundation Pty Ltd, WOTSO Premises, Level 2, 7 Neptune Street, ACT 2606, Australia

[3]Geography and Environment, Jahangirnagar University, Dhaka, Bangladesh

[4]Founder, Gross International Nature

[5]Genofax, Building G, 1G Homebush Bay Drive, Rhodes, NSW-2138, Australia

*Corresponding Author

Abstract

A severe contributor to global warming, Methane (CH4) is a significant element of Green House Gases (GHGs). Both anthropogenic and natural sources are responsible for its emission. The development of satellites for remote sensing has made it convenient to study the spatiotemporal distribution of any gaseous component. Tropospheric Monitoring Instrument (TROPOMI) integrated with Sentinel-5 Precursor (Sentinel-5P) satellite is proven efficient in studying CH4. Sentinel-5P TROPOMI CH4 data from February 2019 to September 2022 has been used to research southwest districts with the Sundarbans mangrove forest. Besides, satellite data from MODIS (Moderate Resolution Imaging Spectroradiometer), ERA5 and Climate Hazards Group Infrared Precipitation with Station data (CHIRPS) are used to analyse methane changes from 2019 to 2022. All these diverse datasets have been retrieved by using Google Earth Engine (GEE) platform. CH4 emission shows an increasing trend over the study area. The emission rate is higher (more than 1900 to 1950 ppb) in all districts during the dry winter season, especially from January to March. Particularly, cropland and water have regular and higher emissions. On the contrary, bare ground and rangeland have irregular and higher emissions. Built area exerts higher emission trend (more than 1900 ppb) in Satkhira district. All districts, including the Sundarbans, have shown positive relation with Normalized Difference Vegetation Index (NDVI) and Normalized Difference Water Index (NDWI),

indicating single cropland and shrimp aquaculture as significant emitters. The presence of massive vegetation and waterbodies in the Sundarbans is responsible for low emissions (below 1900 ppb). Sundarbans have been found with an anomalous correlation with meteorological variables. Apart from the anthropogenic perspective, there could also be potential environmental and geological sources of CH4 emissions.

Keywords: Methane, Sentinel 5P TROPOMI, Land Use Land Cover, South-West Bangladesh, MODIS, ERA5, CHIRPS

Introduction

Methane (CH4) is one of the important greenhouse gas in the atmosphere, after Carbon Dioxide (CO2) (Kozicka et al., 2021; Naik et al., 2021). Its warming potential is 25 times greater than CO2 (Boucher et al., 2009). CH4 can be emitted due to geological and anthropogenic causes (Judd 2000; Etiope & Klusman 2002; Jacob et al., 2016; Jacob et al., 2021). Geological sources include degradation by bacteria, breakdown of complex organic molecules and inorganic processes deep within the earth's crust (Judd 2000). Anthropogenic sources include livestock, oil–gas, landfills, coal mines, wastewater management, and rice cultivation (Jacob et al., 2016). CH4 in the atmosphere is increased three times since the pre-industrial period. Slow CH4 rise between 1984 and 1999 (8.42 ± 0.62 ppb/year), lower CH4 rise between 2000 and 2010 (2.5 ± 0.52 ppb/year), and resumed CH4 surge between 2011 and 2021 (9.46 ± 0.57 ppb/year) (Dlugokencky, 2021). In this industrial era, prolonged emissions of CH4 are caused by anthropogenic or natural/geologic sources, and reduction in the atmospheric oxidative capacity or combined action of all three factors remains unresolved (Nisbet et al., 2019; Turner et al., 2019).

According to Tareq et al. 2022, The Ganges River discharges to mangrove forests which is a hotspot for the study of biogenic gases (CO2, CH4 & N2O) which are radioactively active gases. The Acharya et al. study showed that estuaries are a minor source of CH4 but oscillate between sources and sinks for CO2 and N2O gases through water-air CO2, CH4, and N2O fluxes. It was also found that the CO2 fluxes were ~10 times higher during the monsoon seasons. In an important river in South-West Bangladesh, The Rupsha River metal concentration of As, Pb, Cd and Cr were found in sediment sample which attributed to natural sources and anthropogenic industrial activities (Tareq et al., 2022). Due to river erosion and new alluvial deposition the estuarine islands constantly change shape and position (Ashrafuzzaman et al., 2022a).

The phenomenon as climate change and sea level rise is worsened by the emission of Green House Gases (GHG's). About half of the population lives 5m below sea level, it is estimated that 17% of the territory of Bangladesh will disappear and create 20 million refugees. It has been projected by scientists that in the year 2100 the sea level rise will range from 0.53 to 0.97 m in 37 coastal stations at the Bay of Bengal, where the predicted global sea level rise is 0.09–0.88 m (Haque et al., 2019). The impacts of SLR are worsened by

floods, eroding coastlines, saltwater intrusion, increased storm frequency and ecosystem changes (Ashrafuzzaman et al., 2022b). The residents of the southwestern coastal region of Bangladesh (SWCRB) are trying to adapt to the effects of climate change and sea level rise (CCSLR) as saltwater intrusion, agricultural loss, and high-intensity cyclones (Ashrafuzzaman et al., 2022a)

Eutrophication is the process of deposition of nutrients and minerals such as phosphate and nitrates. This phenomenon hinders aquaculture farmers by changing the biochemical oxygen demand (BOD) and transparency. The agricultural sector is supposed to be the largest emitter of CH4 gas. All the same, CH4 emission varies seasonally depending on agricultural activities and meteorology which is intensive during June-September from agriculture. The CH4 production and oxidation influence fertilization (Schimel 2000). The human impact of CH4 emission induced by agricultural activities can be therefore reduced by biochar–based fertilizers modulating soil biogeochemistry and microbial activity. Spaceborne measurements as AIRS (Atmospheric Infrared Sounder), OCO (Orbiting Carbon Observatory), SCIAMACHY (Scanning Absorption Spectrometer for Atmospheric Cartography), and GOSAT (Greenhouse Gases Observing Satellite) can be used for the study of atmospheric trace gases (Schaefer et al., 2016; Singh et al., 2021).

Geographic Information System (GIS) is an effective tool to represent CH4 emission spatiotemporally. Satellite sensors help to define CH4 content at the global scale (Jacob et al., 2016). CH4 observation from space on a worldwide scale includes various satellite sensors. It started SCIAMACHY instrument (Frankenberg et al., 2005), GOSAT and the TROPOMI (Tropospheric Monitoring Instrument) instrument (Lorente et al., 2021). Satellite-based methane observations have been used to study emission globally, on a continental scale and even on a local/small scale (Alexe et al., 2015; Bergamasch et al., 2013; Wang et al., 2013; Qu et al., 2021; Wecht et al., 2014; Maasakkers et al., 2021; Lu et al., 2022; Miller et al., 2019; Zhang et al., 2020; Shen et al., 2021; Pandey et al., 2019; Sadavarte et al., 2021; Lauvaux et al., 2022; Maasakkers, et al., 2022a,b; Feng et al., 2022). Javadinejad et al. (2019) examined GOSAT-based CH4 emissions with different climatic parameters and observed a significant relationship between them. Among all satellites, TROPOMI is one of the most efficient sensors to monitor CH4, because of high spatial resolution, frequent revisit, time and free availability. It is integrated with Sentinel-5 Precursor (Sentinel-5P), and its data is available from 2019. CH4 content is evaluated using two spectral ranges, i.e., near-infrared (NIR: 675–775 nm) and short-wave infrared (SWIR: 2305–2385 nm) (Hu et al., 2016).

Study Area

The specific area of this study is located southwest region of Bangladesh, covering Satkhira, Khulna, and Bagerhat districts with the UNESCO world heritage site- Sundarbans mangrove forest. It has an Indian province in the west, Barishal district in the east, Jessore district in the south and Bay of Bengal in the north.

The extent of the study area is from 88°54'46.849 "East to 89°50'3.643 "East, from 22°52'53.362 "North to 21°57'47.624"North (Figure 1). Khulna, Satkhira and Bagerhat districts have a total population of 5,780,576 (BBS, 2011). Khulna and Bagerhat districts have a decreasing trend in population from 2001 to 2011 (Table 1). A maximum decrease has occurred in the Bagerhat district, and only the Satkhira district has an increase in population. Elevation ranges from 16 meters below Mean Sea Level (MSL) to 29 meters. The average maximum height (11.45 meters MSL) is in Sarankhola upazila (Bagerhat district), and the minimum elevation (1.89 meters MSL) is in Shyamnagar upazila (Satkhira district) (Figure 1). This area receives a total rainfall of 1750-2000 millimetres annually, and the annual average temperature is from 26° to more than 26.5° Celsius (Barry and Chorley, 2009). A geologically significant portion of this study area comprises Tidal deltaic deposits and Mangrove swamp deposits (Alam et al., 1990; Figure 2a). General soil types are majorly Calcareous Dark Grey Floodplain and Non-calcareous Grey Floodplain (non-saline) (Brammer, 1996; Figure 2b). Apart from the Sundarbans mangrove forest, major land cover classes are cropland (2962.90 sq. km) and water (1630.32 sq. km) until 2021 (Figure 2(d)(e)(f); Table 5). The Sundarbans have the highest amount of vegetation and water bodies (Table 5). Salinity level appears slight to very strong across the middle portion covering Shyamnagar, Kaliganj, Koyra, Dacope, Paikgacha, Rampal, Morelganj upazilas. The southern part of the Satkhira district is non-saline and the southern part of the Bagerhat district is intensely saline (SRDI, 2010; Figure 2c). Single crop (Boro rice) is cultivated in the majority area of agricultural land of Satkhira, Khulna and Bagerhat districts (Table 2, 3). The principal crop after Boro rice is Vegetable, cultivated in cropland and floating gardens (Nowreen et al., 2013; Table 3). Primary fish production comes from Shrimp aquaculture and ponds. Bagerhat district has a considerable fish supply from the Sundarbans area (Table 4). From the physiographic view, the concerned study area holds a unique location, environment and ecosystem in Bangladesh.

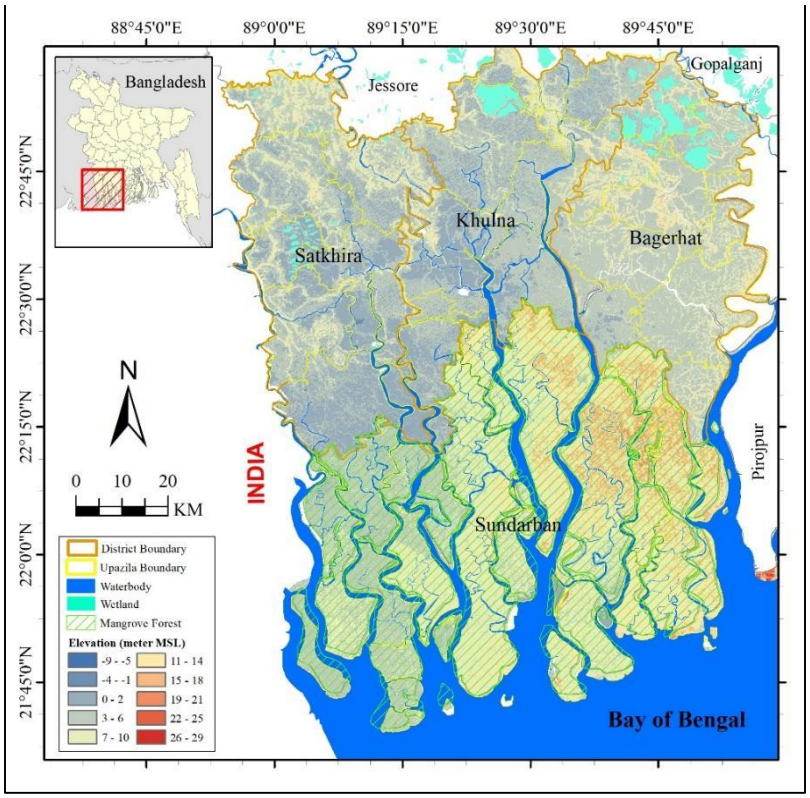

Figure 1: Study Area (South-Western Districts of Bangladesh)

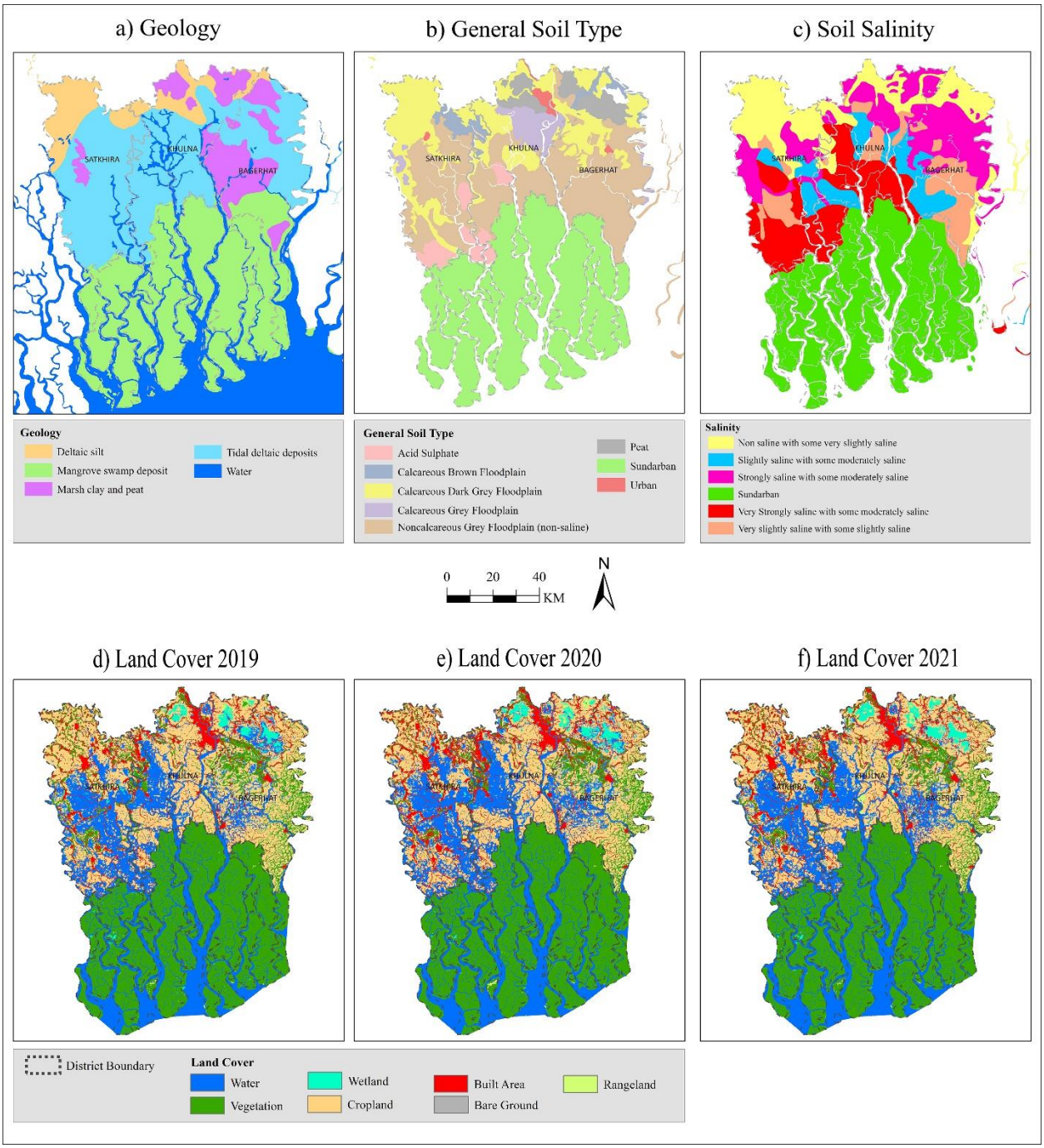

Figure 2: Different Environmental Parameters and Land Cover of the Study Area

Ma et al. (2018) observed that CH4 emissions from inland aquaculture ponds contribute to regional and national GHG (greenhouse gas) budgets. Rosentreter et al. (2021) found that aquatic ecosystem emits half of global CH4. Only coastal aquaculture ponds emit almost 5.9 ± 15.1 Tg (Teragram) CH4/year. Commercial shrimp culture is also included in the aquatic ecosystem (Rosentreter et al., 2021). The conversion of brackish marsh to coastal shrimp pond causes increased emission of CH4, even 10-fold higher

than brackish marsh emission (Yang et al., 2017). To measure CH4 emissions from the shrimp aquaculture area, (Yang et al., 2019) collected water and sediment samples. The middle stage of culture emits a maximum CH4 than the initial and final stages (Yang et al., 2018; Yang et al., 2019). Integrated activities of organic and inorganic processes in shrimp aquaculture are responsible for significant CH4 emissions. The South-west region of Bangladesh is located along a coastal belt with unique land cover and environmental characteristics. Here, coastal aquaculture, especially shrimp in brackish water, is a significant fish production sector (DOF, 2021). On July 2022, fuel gas emission from a shrimp enclosure at Mongla (Bagerhat district) was reported, which was also being used for cooking activity (The Daily Star, 2022). As far as it is known, no study on CH4 emission from this major coastal and aquaculture region of Bangladesh has been conducted yet. So, this study aims to study atmospheric CH4 dynamics of southwest Bangladesh using Sentinel-5 TROPOMI satellite. The specific objectives of this study are to (i) study CH4 emissions from spatial and different land cover dimensions, (ii) find out potential land cover behind CH4 emission, and (iii) relate between CH4 and different meteorological and surface variables. We hypothesise that (i) specific anthropogenic activities emit a significant level of CH4, (ii) as the region is in a unique physiographic division, it may have both geological and climatic factors of CH4 emission. This study's findings would illustrate the scientific basis for refining climate action plans to reduce GHGs (greenhouse gases) on the national, and in turn, international levels.

Table 1: Population Change, 2001-2011 (BBS, 2011)

		2001	2011
Khulna	Urban	1284208	777588
	Rural	1094763	1540939
	Total	2378971	2318527
Bagerhat	Urban	206554	195331
	Rural	1342477	1280759
	Total	1549031	1476090
Satkhira	Urban	171614	197616
	Rural	1693090	1788343
	Total	1864704	1985959

Table 2: Land Utilization Statistics (sq. km) 2019-20 (BBS, 2021)

	Satkhira	Khulna	Bagerhat
Total area	3816.19	4394.89	3957.83
Forest area	1497.34	2209.59	2294.57
Not available for cultivation area	546.33	789.14	348.03
Culturable waste area	68.8	44.52	48.56
Current fallow area	263.05	141.64	169.97

Single cropped area	890.31	752.72	704.15
Double cropped area	428.97	339.94	263.05
Triple cropped area	121.41	117.36	121.41
Quadruple Cropped area	0.00	0.00	8.09
Net cropped area	1440.68	1210.01	1096.70
Gross cropped area	2112.46	1784.67	1626.84

Table 3: Area (sq. km) Irrigated under Different Crops 2019-20 (BBS, 2021)

Region	Aman	Boro	Wheat	Potato	Vegetable	Other Crops	Total Irrigated Area
Satkhira	36.42	712.25	8.09	24.28	174.01	24.28	979.34
Khulna	24.28	598.94	-	8.09	72.84	28.33	732.48
Bagerhat	4.05	424.92	-	4.05	60.70	12.14	505.86

Table 4: District-wise Annual Fish Production (Metric Tons) of Inland Water bodies in 2019-20 (DOF, 2021)

		Satkhira	**Khulna**	**Bagerhat**
River		1380	3666	5318
Sundarbans		716	762	19529
Beel		33	228	32
Flood Plain		12674	19754	5093
Pond		39599	16040	17603
Seasonal waterbody		1761	1022	1779
Baor		201	0	10
Shrimp/Prawn Production	Bagda	24088	12549	17488
	Galda	8631	13325	16337
	other shrimp/prawn	4383	1733	2117

Table 5: Different Land Cover Area (sq. km) of 2019, 2020, and 2021 (Adapted from Karra et al., 2021)

Year		Bagerhat	Khulna	Satkhira	Sundarban	**Total**
Water	***2019***	320.73	583.82	800.45	1557.41	**3262.41**
	2020	331.30	607.49	820.22	1551.49	**3310.50**
	2021	312.53	552.65	765.13	1555.51	**3185.82**
Veg etati	***2019***	397.86	131.56	216.06	3791.00	**4536.48**
	2020	389.68	112.65	134.67	3801.10	**4438.10**

	2021	385.78	115.46	161.46	3798.97	**4461.67**
Wetland	***2019***	57.32	66.52	18.05	10.80	**152.69**
	2020	78.85	79.56	13.04	3.42	**174.87**
	2021	81.42	82.56	8.84	6.76	**179.58**
Cropland	***2019***	1051.58	1034.53	924.81	7.06	**3017.98**
	2020	994.51	960.53	859.93	7.20	**2822.17**
	2021	1010.40	1007.02	945.48	6.54	**2969.44**
Built Area	***2019***	164.59	318.13	332.98	3.04	**818.74**
	2020	197.83	361.64	463.15	3.26	**1025.88**
	2021	199.63	351.58	407.88	3.22	**962.31**
Bare Ground	***2019***	3.17	2.06	0.53	0.56	**6.32**
	2020	2.28	3.03	1.40	0.62	**7.33**
	2021	4.03	6.17	1.97	0.62	**12.79**
Rangeland	***2019***	6.99	14.27	1.05	8.08	**30.39**
	2020	7.79	25.98	1.53	10.86	**46.16**
	2021	8.45	35.44	3.18	6.34	**53.41**

Methods and Data

The study area has four parts: Satkhira, Khulna, Bagerhat district and Mangrove Forest Sundarban of Bangladesh. Sentinel-5 TROPOMI has been used in this study. The used band for CH4 is the column-averaged dry-air mixing ratio of CH4 (in ppb—parts per billion). Data were retrieved from 8 February 2019 to 22 September 2022 using Google Earth Engine (GEE). CH4 from Sentinel-5 TROPOMI has been validated by GOSAT satellite and ground-based TCCON instruments. CH4 images have a spatial resolution of 1 × 1 KM (ESA, 2021). A total of 767 images have been analysed for this study. Due to cloud coverage,

there is also some missing CH4 data on specific dates/months (ESA, 2021). Raster datasets of the column-averaged dry-air mixing ratio of CH4 have been used as the primary component. CH4 raster datasets have been averaged for 2019, 2020, 2021, and 2022. The only exception marked was 2022, which had datasets from January 2022 to September 2022. For the land cover of 2019, 2020 and 2021, raster datasets have been adapted from Sentinel-2 land cover (Karra et al., 2021; Figure 2(d,e,f). Moreover, MODIS (Moderate Resolution Imaging Spectroradiometer) sensor is an essential tool that covers data from both land and ocean over a broad scale. It has 36 different bands, which collect data on the earth after 1 to 2 days. Its image pixel has a resolution from 500 metres to 1 KM for other band datasets. Normalised difference vegetation index (NDVI) from MOD13Q1 band, Normalised Difference Water Index (NDWI) from MOD09GA band and land surface temperature (LST) from MOD11C3 band by MODIS satellite have also been used. NDVI represents vegetation, cropland, and grassland, whereas NDWI correspondence to water, wetland, and flooded surface. Time series of mean air temperature and precipitation for each district/area has been retrieved from ERA5 Copernicus Climate Change Service and Climate Hazards Group InfraRed Precipitation with Station data (CHIRPS) respectively (C3S, 2017; Funk et al., 2014)

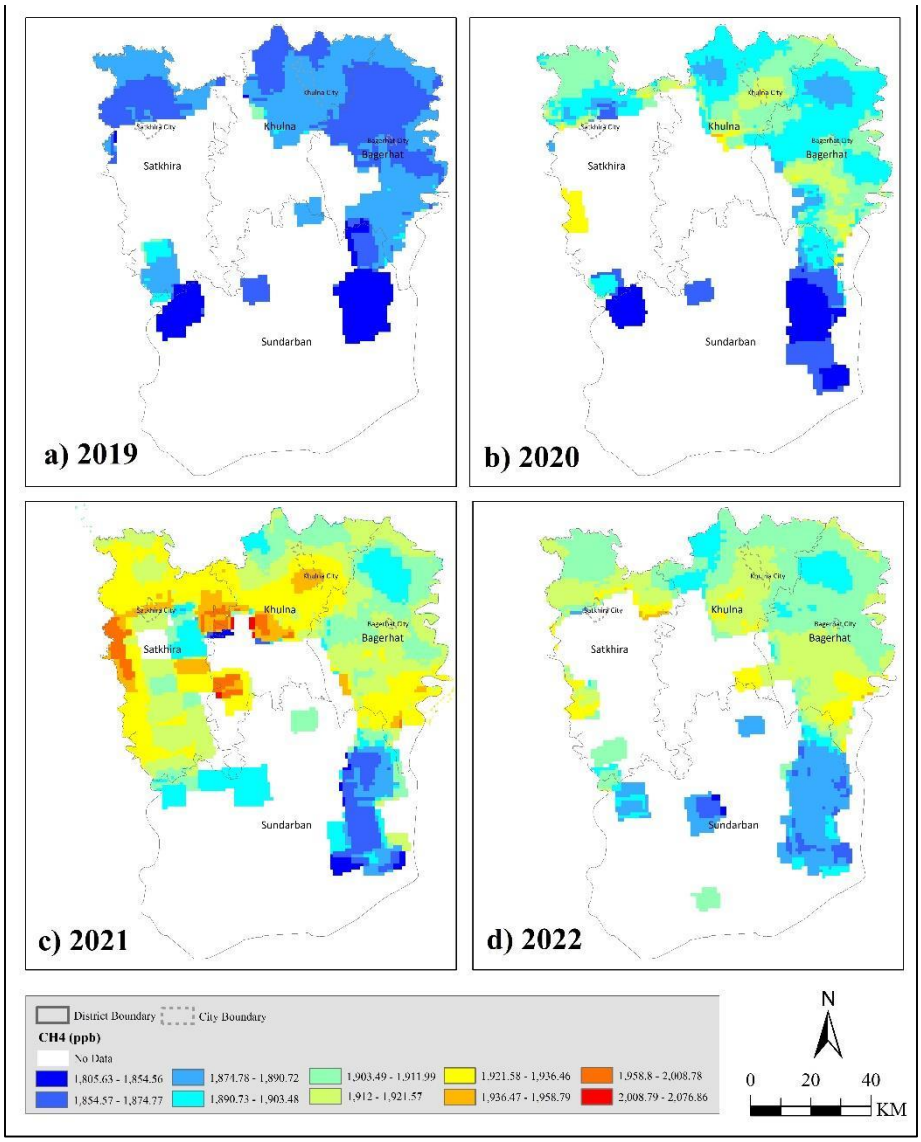

Figure 3: Average CH4 Emission Map by Year

In the study, CH4 time series data for a particular district/boundary has been retrieved to assess temporal change. Zonal statistics have been done using QGIS 3.10 software. First zonal statistics have been calculated to get CH4 distribution statistics within a particular area/boundary. After that, zonal statistics were done between CH4 and land cover raster datasets, revealing CH4 variations over different land covers.

Javadinejad et al. (2019) stated that CH4 emission dynamics impact meteorological/climatic variables. Correlation between the monthly average of CH4 and air temperature, precipitation, LST, NDVI, and NDWI have been done using R (v. 4.1.3). Mean CH4 and other parameter values of each district/boundary over a time series have been used to do Pearson's correlation. The correlation formula is mentioned below:

$$r = \frac{\sum(x_i - \underline{x})(y - \underline{y})}{\sqrt{\sum(x_i - \underline{x})^2 \sum(y_i - \underline{y})^2}}$$

In this formula, each variable has been taken as *x* and *y* representing CH4 count. Pearson's correlation coefficient represents a degree of changes and inter-relational strength between CH4 and each climatic variable.

Result & Discussion

Figure 3 shows Spatio-temporal changes of CH4 over different districts. Among all districts, CH4 emissions increased over Satkhira from 2019 to 2021. The interior of the Sundarban boundary has lower emissions in all years. The statistical variables of the CH4 of different districts are shown in Figure 4a, including average, minimum and maximum values. CH4 raster data is plotted over value and pixel frequency. Khulna district has a full range of CH4 emissions, particularly Paikgacha upazila has the peak emission. Debhata upazila of Satkhira district has remarkable CH4 emission on average. In comparison to the three districts, Sundarban has low CH4 emission and its frequency is also down.

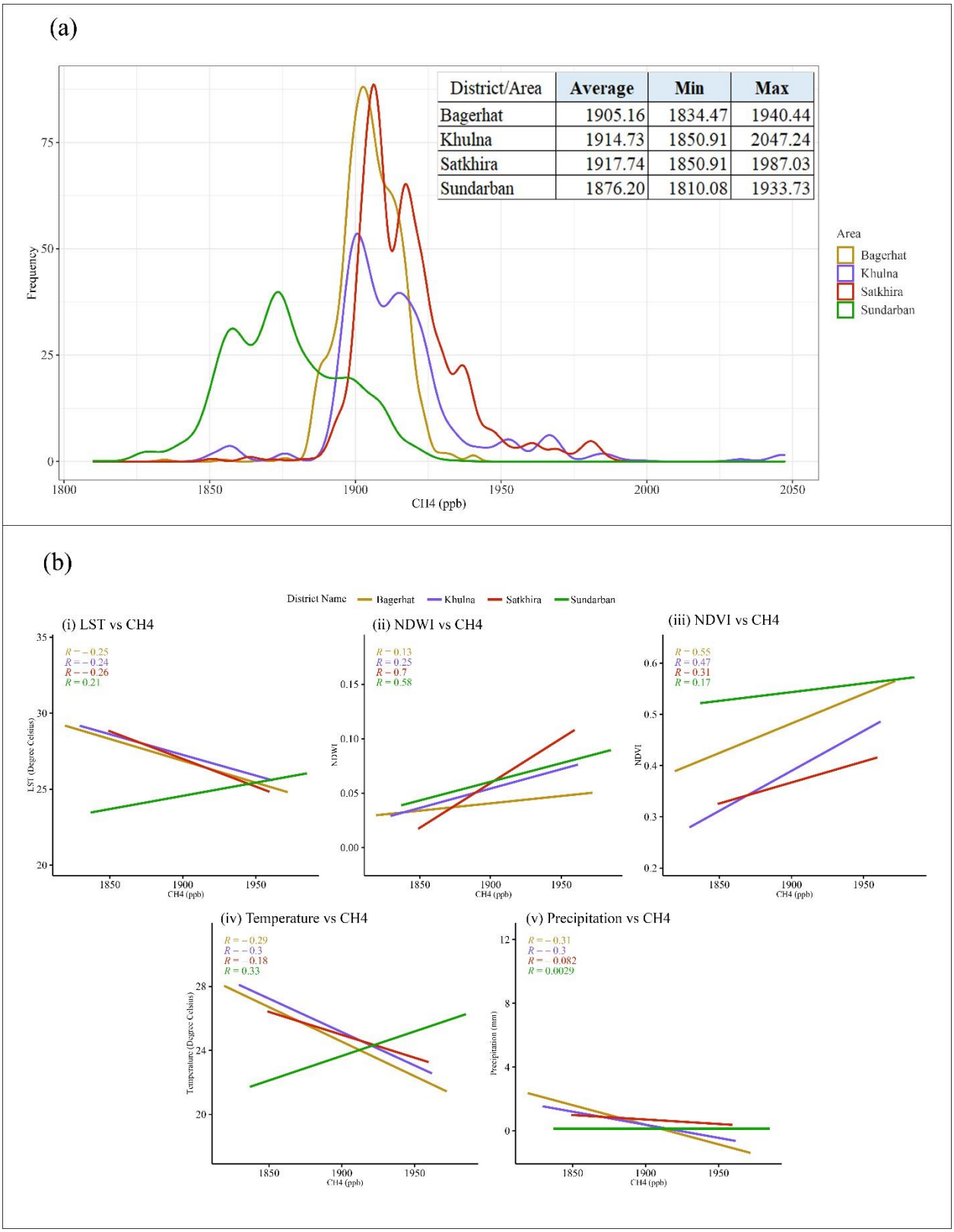

Figure 4: (a) Averaged CH4 Distribution by District, (b) Correlation between Monthly CH4 and Other Parameters

The monthly emission from 2019-2022 of three districts and Sundarban is plotted in Figure 5. Some dates/months do not have CH4 data due to cloudiness in the middle of the year, especially during monsoon season (ESA, 2021). CH4 emission is increasing at particular months (especially the dry winter season) than the previous year. Both Khulna and Bagerhat had continuous CH4 increases from January to March. Besides, Satkhira and Sundarbans have similar trends from January to March and December to March, respectively (Figure 5(c)(d)).

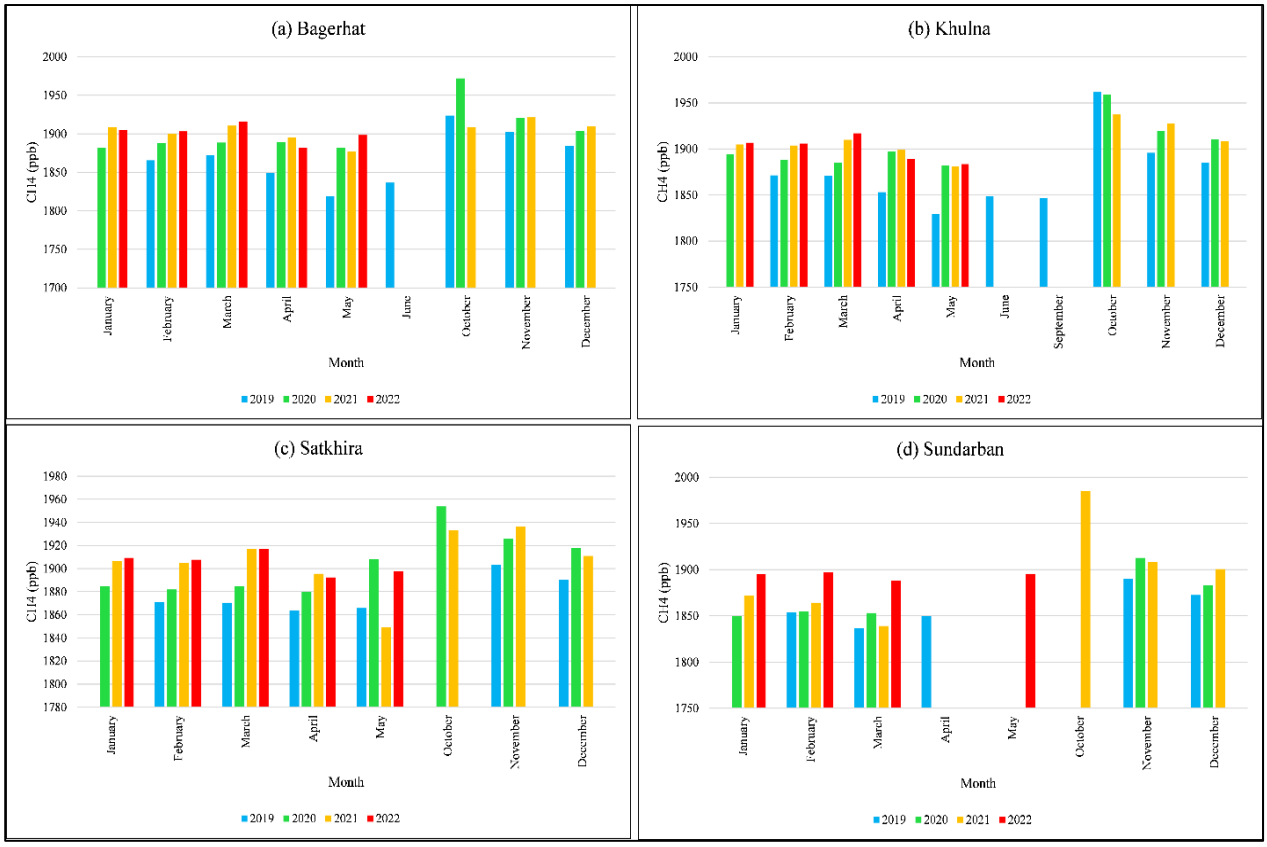

Figure 5: Monthly CH4 Change of Different Areas (2019-2022)

Figure 6(a)(b)(c) show comparatively irregular and higher CH4 emissions from bare ground and rangeland. The bare ground represents brick kilns and heavy industries, potential CH4 emitters (Khan and Paul, 2021). Most brick kilns are situated in Koyra, Dumuria, Rupsa (Khulna district), Satkhira sadar, Kaliganj, Assasuni (Satkhira district). As Mongla seaport is located in this region, many industries in Rampal upazila (Bagerhat) are built on the bank of Mongla river. The geographic location of navigation opportunities in this region is a significant cause behind the development of seaports and industries. Rangeland is fallow land seasonally used for crop cultivation and aquaculture. Cropland and water show an increasing trend of CH4 in three districts. CH4 emissions from cropland can be interpreted as follows, single crop practice,

majorly boro rice cultivation (Table 2, 3). Aquaculture, especially shrimp culture, is being done over a massive area of water and wetland. Seasonally it is also cultured in cropland with rice (Barmon et al., 2004). As coastal aquaculture is regarded as a source of CH4, this major shrimp aquaculture also causes emissions from the cultured area (Ma et al., 2018; Rosentreter et al., 2021). CH4 emission from built areas seems to have an irregular trend in all districts except Satkhira. By 2021 in Sundarban, CH4 from cropland and built area emits CH4 more than 1900 ppb (Figure 6d). Vegetation from everywhere shows an emission level below 1900 ppb. Apart from anthropogenic factors, natural biogeochemical and geological processes in the coastal region could release CH4 into the atmosphere (Arai et al., 2021; The Daily Star, 2022).

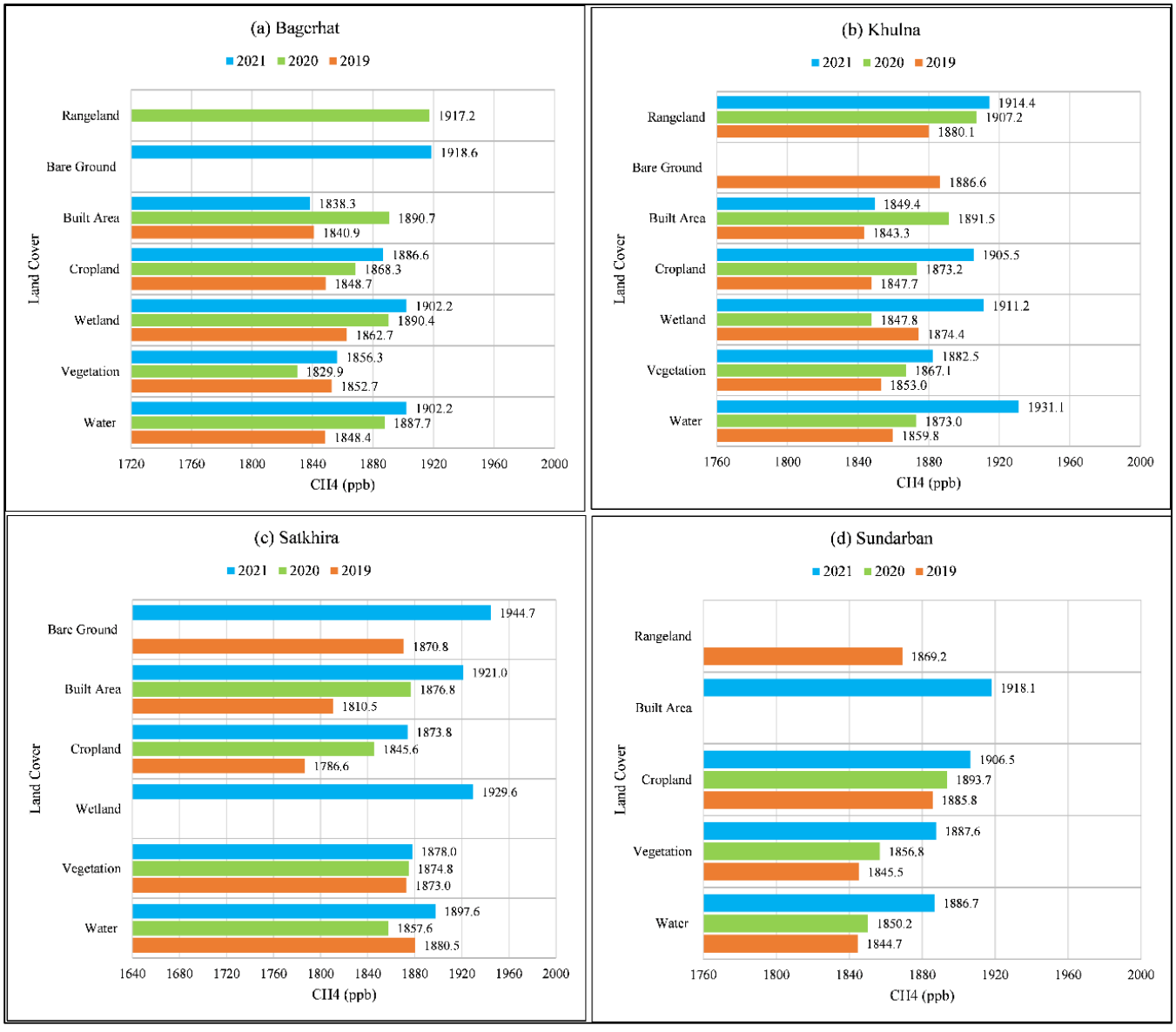

Figure 6: Average CH4 Distribution over Different Land Cover (2019-2021)

After preliminary statistical analysis, as shown in Figure 4a, 5, and 6, it is essential to understand a more precise CH4 relationship. Pearson's correlation was done to interpret the relationship between CH4 and the meteorological-surface parameter. Each variable has been averaged by month from February 2019 to August 2022. Meteorological parameters include temperature (°C), precipitation (millimetre) and surface parameters include LST (°C), NDWI, and NDVI (Figure 4b).

As shown in Figure 4b (i), CH4 has weak negative relation with LST in all areas except in Sundarbans. All areas exhibit positive relations with NDWI (Figure 4b (ii)), where Satkhira has strong, Sundarbans has moderate, Bagerhat and Khulna have weak relations. CH4 emission from coastal aquaculture is verified from this positive relation with NDWI. Bagerhat and Khulna exhibit middle positive relations with NDVI (Figure 4b (iii)), whereas Satkhira and Sundarbans have weak positive relations. Cultivation of rice in most cropland is a possible reason for such emission relation with NDVI (Table 2, 3, 5). In three districts, CH4 has a weak negative association with temperature (Figure 4b (iv)). Except for Sundarbans, other areas tend to be negatively related to precipitation, which is lower than those found in similar studies (Figure 4b (v); Javadinejad et al., 2019). Only in the Sundarbans, CH4 has a weak positive relation with LST, temperature and a fragile positive association with precipitation (Figure 4b (i)(iv)(v)).

Conclusion

The aforementioned study shows that each area has an increasing trend of CH4, especially in the dry winter season. Significant CH4 emissions are observed from cropland and water, as these are dominant land cover in all three districts. Integrated single-crop rice cultivation and shrimp aquaculture are essential factors. Moreover, excessive brick kilns and industries near cities and seaports also trigger emissions. A weak association has been found with CH4 regarding surface feature parameters like NDVI and NDWI, which validates emission from shrimp enclosure and rice field hypothesis. Due to extensive coastal aquaculture, CH4 has a strong relation (0.7) with NDWI in Satkhira (Table 4). Positive relation with NDVI in the coastal region is also reported by Javadinejad et al. (2019). CH4 emission from crops, especially rice fields, is a proven fact. But in recent decades, several studies have found CH4 emission from aquaculture in many coastal regions of the world (Ma et al., 2018; Rosentreter et al., 2021); Yang et al., 2017; Yang et al., 2019). LST, temperature and precipitation have behaved weakly negative for all districts. Only in the Sundarbans, CH4 has a weak to moderate positive relationship with all parameters. There are some anomalies have been observed for LST and temperature. Similarly, LST showed an anomalous trend in a study on Khulna (Dewan et al., 2021). Apart from human-induced activities, there can be possible geological emission causes, as reported in a report before (The Daily Star, 2022).

In the near future, the findings of this study are expected to prove efficient for further work given climate change. The study illustrates the scenario of CH4 emission on a regional scale to progress the UN's

sustainable development goals (SDGs) achievement. It will be a prospective field to study this region's biometeorological and microclimatic dynamics in the coming days.

References

1) Alam, M. K., Hasan, A. S., Khan, M. R., Whitney, J. W., Abdullah, S. K. M., & Queen, J. E. (1990). *Geological map of Bangladesh*. Geological Survey of Bangladesh.

2) Alexe, M., Bergamaschi, P., Segers, A., Detmers, R., Butz, A., Hasekamp, O., Guerlet, S., Parker, R., Boesch, H., Frankenberg, C.J.A.C., Scheepmaker, R.A., Dlugokencky, E., Sweeney, C., Wofsy, S. C., & Kort, E. A. (2015). Inverse modelling of CH 4 emissions for 2010–2011 using different satellite retrieval products from GOSAT and SCIAMACHY. *Atmospheric Chemistry and Physics*, *15*(1), 113-133.

3) Arai, H., Inubushi, K., & Chiu, C. Y. (2021). Dynamics of Methane in Mangrove Forest: Will It Worsen with Decreasing Mangrove Forests?. *Forests*, *12*(9), 1204.

4) Ashrafuzzaman, M., Gomes, C., & Guerra, J. (2022a). Climate justice for the southwestern coastal region of Bangladesh. *Frontiers in Climate*, *4*, art-n.

5) Ashrafuzzaman, M., Santos, F. D., Dias, J. M., & Cerdà, A. (2022b). Dynamics and Causes of Sea Level Rise in the Coastal Region of Southwest Bangladesh at Global, Regional, and Local Levels. *Journal of Marine Science and Engineering*, *10*(6), 779.

6) Barmon, B. K., Kondo, T., & Osanami, F. (2004). Impact of rice-prawn gher farming on agricultural and household income in Bangladesh: a case study of Khulna district. *Journal of Bangladesh Studies*, *6*(1&2), 51-61.

7) Barry, R. G., & Chorley, R. J. (2009). *Atmosphere, weather and climate*. Routledge.

8) BBS (Bangladesh Bureau of Statistics). (2011). Statistical Yearbook of Bangladesh. Statistics Division, Ministry of Planning, Government of the People's Republic of Bangladesh

9) BBS (Bangladesh Bureau of Statistics). (2021). Statistical Yearbook of Bangladesh. Statistics Division, Ministry of Planning, Government of the People's Republic of Bangladesh

10) Bergamaschi, P., Houweling, S., Segers, A., Krol, M., Frankenberg, C., Scheepmaker, R. A., ... & Gerbig, C. (2013). Atmospheric CH4 in the first decade of the 21st century: Inverse modeling analysis using SCIAMACHY satellite retrievals and NOAA surface measurements. *Journal of Geophysical Research: Atmospheres*, *118*(13), 7350-7369.

11) Boucher, O., Friedlingstein, P., Collins, B., & Shine, K. P. (2009). The indirect global warming potential and global temperature change potential due to methane oxidation. *Environmental Research Letters*, *4*(4), 044007.

12) Brammer, H. (1996). The Geography of Soils of Bangladesh, University Pub. *Ltd., Dhaka*.

13) C3S (Copernicus Climate Change Service). (2017). ERA5: Fifth generation of ECMWF atmospheric reanalyses of the global climate. Copernicus Climate Change Service Climate Data Store (CDS). Retrieved from https://cds.climate.copernicus.eu/cdsapp#!/home

14) Dewan, A., Kiselev, G., Botje, D., Mahmud, G. I., Bhuian, M. H., & Hassan, Q. K. (2021). Surface urban heat island intensity in five major cities of Bangladesh: Patterns, drivers and trends. *Sustainable Cities and Society*, *71*, 102926.

15) Dlugokencky, E. J. (2021). Trends in Atmospheric Methane. Retrieved from www.esrl.noaa.gov/gmd/ccgg/trends_ch4/

16) DOF (Department of Fisheries). (2021). Fisheries Statistical Yearbook of Bangladesh 2019-20. Ministry of Fisheries and Livestock, Government of the People's Republic of Bangladesh

17) Etiope, G., & Klusman, R. W. (2002). Geologic emissions of methane to the atmosphere. *Chemosphere*, *49*(8), 777-789.

18) European Space Agency (ESA). (2021). Copernicus Sentinel-5P, TROPOMI Level 2 Methane Total Column products. Version 02. *European Space Agency*. https://doi.org/10.5270/S5P-3lcdqiv

19) Feng, L., Palmer, P. I., Zhu, S., Parker, R. J., & Liu, Y. (2022). Tropical methane emissions explain large fraction of recent changes in global atmospheric methane growth rate. *Nature communications*, *13*(1), 1-8.

20) Frankenberg, C., Platt, U., & Wagner, T. (2005). Iterative maximum a posteriori (IMAP)-DOAS for retrieval of strongly absorbing trace gases: Model studies for CH4 and CO2 retrieval from near infrared spectra of SCIAMACHY onboard ENVISAT. *Atmospheric Chemistry and Physics*, *5*(1), 9-22.

21) Funk, C. C., Peterson, P. J., Landsfeld, M. F., Pedreros, D. H., Verdin, J. P., Rowland, J. D., ... & Verdin, A. P. (2014). A quasi-global precipitation time series for drought monitoring. *US Geological Survey data series*, *832*(4), 1-12.

22) Haque, M., Alam, M., Moniruzzaman, S., & Hoque, M. (2019). The Impact of Climate Change in the Coastal Areas of Bangladesh Affected by Cyclone Bulbul. *Bangladesh J. Ext. Educ*, *1011*, 3916.

23) Hu, H., Hasekamp, O., Butz, A., Galli, A., Landgraf, J., Aan de Brugh, J., ... & Aben, I. (2016). The operational methane retrieval algorithm for TROPOMI. *Atmospheric Measurement Techniques*, *9*(11), 5423-5440.

24) Jacob, D. J., Turner, A. J., Maasakkers, J. D., Sheng, J., Sun, K., Liu, X., ... & Frankenberg, C. (2016). Satellite observations of atmospheric methane and their value for quantifying methane emissions. *Atmospheric Chemistry and Physics*, *16*(22), 14371-14396.

25) Jacob, D. J., Varon, D. J., Cusworth, D. H., Dennison, P. E., Frankenberg, C., Gautam, R., ... & Duren, R. M. (2022). Quantifying methane emissions from the global scale down to point sources using satellite observations of atmospheric methane. *Atmospheric Chemistry and Physics Discussions*, 1-44.

26) Javadinejad, S., Eslamian, S., & Ostad-Ali-Askari, K. (2019). Investigation of monthly and seasonal changes of methane gas with respect to climate change using satellite data. *Applied Water Science*, *9*(8), 1-8.

27) Judd, A. G. (2000). Geological sources of methane. In *Atmospheric Methane* (pp. 280-303). Springer, Berlin, Heidelberg.

28) Karra, K., Kontgis, C., Statman-Weil, Z., Mazzariello, J. C., Mathis, M., & Brumby, S. P. (2021, July). Global land use/land cover with Sentinel 2 and deep learning. In *2021 IEEE international geoscience and remote sensing symposium IGARSS* (pp. 4704-4707). IEEE.

29) Khan, M. A. U., & Paul, A. (2021). Brick Kiln's Green House Gas (GHG) emission and public health perspectives: A study in Chattogram, Bangladesh. *Bangladesh Journal of Environmental Research*, *12*, 50-61.

30) Kozicka, K., Gozdowski, D., & Wójcik-Gront, E. (2021). Spatial-Temporal Changes of Methane Content in the Atmosphere for Selected Countries and Regions with High Methane Emission from Rice Cultivation. *Atmosphere*, *12*(11), 1382.

31) Lauvaux, T., Giron, C., Mazzolini, M., d'Aspremont, A., Duren, R., Cusworth, D., ... & Ciais, P. (2022). Global assessment of oil and gas methane ultra-emitters. *Science*, *375*(6580), 557-561.

32) Lorente, A., Borsdorff, T., Butz, A., Hasekamp, O., Schneider, A., Wu, L., ... & Landgraf, J. (2021). Methane retrieved from TROPOMI: improvement of the data product and validation of the first 2 years of measurements. *Atmospheric Measurement Techniques*, *14*(1), 665-684.

33) Lu, X., Jacob, D. J., Wang, H., Maasakkers, J. D., Zhang, Y., Scarpelli, T. R., ... & Andrews, A. (2022). Methane emissions in the United States, Canada, and Mexico: evaluation of national methane emission inventories and 2010–2017 sectoral trends by inverse analysis of in situ (GLOBALVIEWplus CH 4 ObsPack) and satellite (GOSAT) atmospheric observations. *Atmospheric Chemistry and Physics*, *22*(1), 395-418.

34) Ma, Y., Sun, L., Liu, C., Yang, X., Zhou, W., Yang, B., ... & Li Liu, D. (2018). A comparison of methane and nitrous oxide emissions from inland mixed-fish and crab aquaculture ponds. *Science of the Total Environment*, *637*, 517-523.

35) Maasakkers, J. D., Jacob, D. J., Sulprizio, M. P., Scarpelli, T. R., Nesser, H., Sheng, J., ... & Parker, R. J. (2021). 2010–2015 North American methane emissions, sectoral contributions, and trends:

a high-resolution inversion of GOSAT observations of atmospheric methane. *Atmospheric Chemistry and Physics*, *21*(6), 4339-4356.

36) Maasakkers, J. D., Omara, M., Gautam, R., Lorente, A., Pandey, S., Tol, P., ... & Aben, I. (2022a). Reconstructing and quantifying methane emissions from the full duration of a 38-day natural gas well blowout using space-based observations. *Remote Sensing of Environment*, *270*, 112755.

37) Maasakkers, J. D., Varon, D. J., Elfarsdóttir, A., McKeever, J., Jervis, D., Mahapatra, G., ... & Aben, I. (2022b). Using satellites to uncover large methane emissions from landfills. *Science advances*, *8*(31), eabn9683.

38) Miller, S. M., Michalak, A. M., Detmers, R. G., Hasekamp, O.P., Bruhwiler, L. M. P., & Schwietzke, S. (2019). China's coal mine methane regulations have not curbed growing emissions, *Nature Community* 10, 303, 865. https://doi.org/10.1038/s41467-018-07891-7

39) Naik, V., Szopa, S., Adhikary, B., Artaxo, P., Berntsen, T., Collins, W. D., ... & Zanis, P. (2021). Short-lived climate forcers. *Climate Change*.

40) Nisbet, E. G., Manning, M. R., Dlugokencky, E. J., Fisher, R. E., Lowry, D., Michel, S. E., ... & White, J. W. (2019). Very strong atmospheric methane growth in the 4 years 2014–2017: Implications for the Paris Agreement. *Global Biogeochemical Cycles*, *33*(3), 318-342.

41) Nowreen, S., BinteMurshed, S., Saiful Islam, A. K. M., AlfiHasan, M., & Kumar Sarker, T. (2013). An Indicator of Climate Change in the South West Region of Bangladesh. *International Journal of Climate Change: Impacts & Responses*, *4*(3).

42) Pandey, S., Gautam, R., Houweling, S., Van Der Gon, H. D., Sadavarte, P., Borsdorff, T., ... & Aben, I. (2019). Satellite observations reveal extreme methane leakage from a natural gas well blowout. *Proceedings of the National Academy of Sciences*, *116*(52), 26376-26381.

43) Parker, R. J., Webb, A., Boesch, H., Somkuti, P., Barrio Guillo, R., Di Noia, A., ... & Wunch, D. (2020). A decade of GOSAT Proxy satellite CH 4 observations. *Earth System Science Data*, *12*(4), 3383-3412.

44) Qu, Z., Jacob, D. J., Shen, L., Lu, X., Zhang, Y., Scarpelli, T. R., ... & Delgado, A. L. (2021). Global distribution of methane emissions: a comparative inverse analysis of observations from the TROPOMI and GOSAT satellite instruments. *Atmospheric Chemistry and Physics*, *21*(18), 14159-14175.

45) Rosentreter, J. A., Borges, A. V., Deemer, B. R., Holgerson, M. A., Liu, S., Song, C., ... & Eyre, B. D. (2021). Half of global methane emissions come from highly variable aquatic ecosystem sources. *Nature Geoscience*, *14*(4), 225-230.

46) Sadavarte, P., Pandey, S., Maasakkers, J. D., Lorente, A., Borsdorff, T., Denier van der Gon, H., ... & Aben, I. (2021). Methane emissions from superemitting coal mines in Australia quantified using TROPOMI satellite observations. *Environmental Science & Technology*, *55*(24), 16573-16580.

47) Sha, M. K., Langerock, B., Blavier, J. F. L., Blumenstock, T., Borsdorff, T., Buschmann, M., ... & Zhou, M. (2021). Validation of methane and carbon monoxide from Sentinel-5 Precursor using TCCON and NDACC-IRWG stations. *Atmospheric Measurement Techniques*, *14*(9), 6249-6304.

48) Shen, L., Zavala-Araiza, D., Gautam, R., Omara, M., Scarpelli, T., Sheng, J., ... & Jacob, D. J. (2021). Unravelling a large methane emission discrepancy in Mexico using satellite observations. *Remote Sensing of Environment*, *260*, 112461.

49) Singh, A., Kuttippurath, J., Abbhishek, K., Mallick, N., Raj, S., Chander, G., & Dixit, S. (2021). Biogenic link to the recent increase in atmospheric methane over India. *Journal of Environmental Management*, *289*, 112526.

50) SRDI. (2010). Saline Soils of Bangladesh. Soil Resources Development Institute. Dhaka.

51) Tareq, S. M., Lu, X. X., Shammi, M., & Maruo, M. (2022). Hydrobiogeochemistry of major Asian rivers. *Frontiers in Earth Science*, *10*.

52) The Daily Star. (2022, 2 July). Gas spewing out from fish enclosure in Bagerhat, being used for cooking by landowner. Retrieved 6 August, 2022, from https://www.thedailystar.net/environment/natural-resources/energy/news/gas-spewing-out-fish-enclosure-bagerhat-being-used-cooking-landowner-3062001

53) Turner, A. J., Frankenberg, C., & Kort, E. A. (2019). Interpreting contemporary trends in atmospheric methane. *Proceedings of the National Academy of Sciences*, *116*(8), 2805-2813.

54) Wang, F., Maksyutov, S., Tsuruta, A., Janardanan, R., Ito, A., Sasakawa, M., ... & Matsunaga, T. (2019). Methane emission estimates by the global high-resolution inverse model using national inventories. *Remote Sensing*, *11*(21), 2489.

55) Wecht, K. J., Jacob, D. J., Frankenberg, C., Jiang, Z., & Blake, D. R. (2014). Mapping of North American methane emissions with high spatial resolution by inversion of SCIAMACHY satellite data. *Journal of Geophysical Research: Atmospheres*, *119*(12), 7741-7756.

56) Yang, P., Bastviken, D., Lai, D. Y. F., Jin, B. S., Mou, X. J., Tong, C., & Yao, Y. C. (2017). Effects of coastal marsh conversion to shrimp aquaculture ponds on CH4 and N2O emissions. *Estuarine, Coastal and Shelf Science*, *199*, 125-131.

57) Yang, P., Lai, D. Y., Yang, H., Tong, C., Lebel, L., Huang, J., & Xu, J. (2019). Methane dynamics of aquaculture shrimp ponds in two subtropical estuaries, southeast China: dissolved

concentration, net sediment release, and water oxidation. *Journal of Geophysical Research: Biogeosciences*, *124*(6), 1430-1445.

58) Yang, P., Zhang, Y., Lai, D. Y., Tan, L., Jin, B., & Tong, C. (2018). Fluxes of carbon dioxide and methane across the water–atmosphere interface of aquaculture shrimp ponds in two subtropical estuaries: The effect of temperature, substrate, salinity and nitrate. *Science of the Total Environment*, *635*, 1025-1035.

59) Zhang, Y., Gautam, R., Pandey, S., Omara, M., Maasakkers, J. D., Sadavarte, P., ... & Jacob, D. J. (2020). Quantifying methane emissions from the largest oil-producing basin in the United States from space. *Science advances*, *6*(17), eaaz5120.

60) Zhao, R., Li, Y., & Ma, M. (2021). Mapping paddy rice with satellite remote sensing: a review. *Sustainability*, *13*(2), 503.